

# Oxidative potential in rural, suburban and city centre atmospheric environments in Central Europe

Máté Vörösmarty<sup>1</sup>, Gaëlle Uzu<sup>2</sup>, Jean-Luc Jaffrezo<sup>2</sup>, Pamela Dominutti<sup>2</sup>, Zsófia Kertész<sup>3</sup>, Enikő Papp<sup>3</sup>,  
and Imre Salma<sup>4</sup>

<sup>1</sup> Hevesy György Ph. D. School of Chemistry, ELTE Eötvös Loránd University, Budapest, Hungary

<sup>2</sup> University of Grenoble Alps, IRD, CNRS, INRAE, Grenoble, France

<sup>3</sup> Laboratory for Heritage Science, Institute for Nuclear Research, Debrecen, Hungary

<sup>4</sup> Institute of Chemistry, ELTE Eötvös Loránd University, Budapest, Hungary

**Correspondence:** Imre Salma (salma.imre@ttk.elte.hu)

**Abstract.** Oxidative potential (OP) is an emerging health-related metric which integrates several physicochemical properties of particulate matter (PM) that are involved in the pathogenesis of the diseases resulting from the exposure to PM. Daily PM<sub>2.5</sub>-fraction aerosol samples collected in the rural background of the Carpathian Basin and in the suburban area and centre of its largest city of Budapest in each season over one year were utilised to study the OP at the related locations for the first time. The samples were analysed for particulate matter mass, main carbonaceous species, levoglucosan and 20 chemical elements. The resulted data sets were subjected to positive matrix factorisation to derive the main aerosol sources. Biomass burning (BB), suspended dust, road traffic, oil combustion mixed with coal combustion and long-range transport, vehicle metal wear and mixed industrial source were identified. The OP of the sample extracts in simulated lung fluid was determined by ascorbic acid (AA) and dithiothreitol (DTT) assays. The comparison of the OP data sets revealed some differences in the sensitivities of the assays. In the heating period, both the OP and PM mass levels were higher than in spring and summer, but there was a clear misalignment between them. In addition, the heating period-to-non-heating period OP ratios in the urban locations were larger than for the rural background by factors of 2–4. The OP data sets were attributed to the main aerosol sources using multiple linear regression with the weighted least squares approach. The OP was unambiguously dominated by BB at all sampling locations in winter and autumn. The joint effects of motor vehicles involving the road traffic and vehicle metal wear played the most important role in summer and spring, with considerable contributions from oil combustion and resuspended dust. In winter, there is temporal coincidence between the most severe daily PM health limit exceedances in the whole Carpathian Basin and the chemical PM composition causing larger OP. Similarly, in spring and summer, there is a spatial coincidence in Budapest between the urban hotspots of OP-active aerosol constituents from traffic and the high population density in central quarters. These features offer possibilities for more efficient season-specific air quality regulations focusing on well-selected aerosol sources or experimentally determined OP rather than on PM mass in general.

## 34 **1 Introduction and objectives**

35 Poor air quality caused by high concentrations of particulate matter (PM) is one of the most severe public  
36 health concerns for humans worldwide (e.g. Lelieveld et al., 2015, 2020; Bondy, 2016; Cohen et al.,  
37 2017). Its acute and chronic effects, such as lung, cardiovascular and cerebrovascular diseases have been  
38 documented in both epidemiological and toxicological studies (e.g. Donaldson et al., 2005; Valavanidis  
39 et al., 2008; Apte et al., 2015; Riediker et al., 2019; Kelly and Fussell, 2020).

40

41 Due to the chemical, physical and biological complexity of ambient aerosol particles, their dynamic  
42 character and possible synergisms among air pollutants, a sophisticated interplay of multiple factors is  
43 involved in the pathogenesis of the diseases resulting from the exposure to PM. The main factors can  
44 involve: 1) mass concentrations of PM<sub>2.5</sub> or PM<sub>10</sub> size fractions, 2) amounts of potentially toxic chemical  
45 components such as transition and heavy metals, polycyclic aromatic hydrocarbons (PAHs), soot and  
46 specific organics, 3) certain chemical speciation forms such as Cr(VI) versus Cr(III), 4) lung  
47 bioaccessibility of critical constituents, 5) surface reactivity of particles, 6) number concentrations of very  
48 small particles such as ultrafine particles or engineered nanomaterials, 7) shape and morphology of  
49 particles such as for asbestos or silica and 8) active components of biogenic origin such as bacteria,  
50 viruses, pollens and moulds or with radioactivity such as radon progeny (Riediker et al., 2019). Therefore,  
51 it cannot be expected that a single or a few aerosol metrics broadly express the induced biological  
52 responses. In the first approximation, PM mass is often selected from these factors as a simplistic metric,  
53 and it can be refined by further particle properties.

54

55 One of the most important biological mechanisms by which PM induces adverse health effects is causing  
56 an oxidant-antioxidant imbalance in the respiratory system at the cellular level (Kelly and Mudway, 2003;  
57 Borm et al., 2007; Kelly and Fussell, 2012, 2015; Cassee et al., 2013; Valavanidis et al., 2013; Janssen et  
58 al., 2014). This is called as oxidative stress. It is related to 1) stimulating cells to uncontrolled production  
59 of excess reactive oxygen species (ROS) endogenously, e.g. directly by Fenton-type reactions of redox-  
60 active aerosol components in the human body or indirectly through biotransformation, e.g. of PAHs or 2)  
61 inefficient elimination of ROS by the antioxidant defence system of the body. These can lead to  
62 inflammatory processes that increase the risk for various diseases and can result in biological aging and  
63 apoptosis (Ayres et al., 2008; Verma et al., 2012; Gao et al., 2020). The capacity of PM to invoke oxidative  
64 stress is quantified by its oxidative potential (OP). This integrates several factors of the particle properties  
65 1–8 listed above. Numerous epidemiological studies suggest that the OP can be one of the central  
66 quantities that is responsible for several health endpoints including specific acute effects such as

67 emergency treatment of asthma and congestive heart failure and that largely explains the underlying  
68 biological bases of toxicity (e.g. Bates et al., 2015; Kelly and Fussel, 2015; Abrams et al., 2017; Yue et  
69 al., 2018; Weichenthal et al., 2019; Daellenbach et al., 2020; Dhalla et al., 2000; Zhang et al., 2022;  
70 Baumann et al., 2023).

71  
72 As a result, there has been a substantial and increasing scientific interest in the measurement  
73 improvements of OP using (biological) in vivo, in vitro cellular and in vitro acellular assays, and in the  
74 identification of the aerosol components and sources closely related to OP (e.g. Cho et al., 2005; Künzli  
75 et al., 2006; Boogaard et al., 2012; Verma et al., 2014, 2015; Kelly and Fussel, 2015; Fang et al., 2016;  
76 Calas et al., 2017; Weber et al., 2018; Shahpoury et al., 2021; Borlaza et al., 2021b, 2022; Lionetto et al.,  
77 2021; Zhang et al., 2022). The OP is frequently measured by acellular assays for exogenous ROS, in  
78 which the PM extract or the particles directly cause a consumption rate of some antioxidants such as  
79 ascorbic acid (AA) or of some chemical surrogates to cellular reducing agents, e.g. dithiothreitol (DTT).  
80 The quantifications are generally based on spectrophotometry. More sophisticated detection methods  
81 which directly determine the ROS production are also available (Katerji et al., 2019).

82  
83 The most frequently used assays were compared for PM<sub>10</sub>-fraction aerosol samples considering the  
84 chemical composition of particles as well (Calas et al., 2018; Lionetto et al., 2021; Shahpoury et al.,  
85 2022). It was concluded that the assays correlated with each other but were not equivalent. All assays  
86 were somewhat specific, and no consensus has been reached on the “best assay” nor on a standardised  
87 methodology for each assay (Weber et al., 2021; Zhang et al., 2022). At the same time, it seems sensible  
88 to compare the results obtained by an identical sample preparation and OP measurement method for  
89 different environmental types. Likewise, comparing the data derived by different experimental methods  
90 applied to similar sample types can contribute to revealing and understanding the different properties or  
91 characteristics of these methods for various chemical components and sources. Both approaches can also  
92 yield considerable methodological development.

93  
94 The main common features of the assays are that 1) they exhibit different responses to various groups of  
95 ROS-generating compounds and their bioavailability, 2) their sensitivity depends on the partner reaction  
96 compound to ROS, and 3) they show nonlinear response to PM mass concentration (Charrier et al., 2016;  
97 Fang et al., 2016; Calas et al., 2017; Shahpoury et al., 2021). A large number of PM constituents were  
98 identified to influence the OP. The DTT assay responds sensitively to ROS produced by organic  
99 compounds and indirectly by soluble transition metals, mainly Cu(II), Mn(II) and Fe(II), and can be also  
100 influenced by synergetic or antagonistic effects between some chemical components (Charrier and

101 Anastasio, 2012; Bates et al., 2019; Shahpoury et al., 2021; Borlaza et al., 2022). The AA assay was  
102 shown to express large sensitivity to transition metals and some specific organics such as quinones  
103 (Künzli et al., 2006; Godri et al., 2011; Visentin et al., 2016).

104

105 It is important to extend the studies on this emerging health-related metric to cities and regions in the  
106 world. The knowledge on the OP for a large part of Central Europe, namely the Carpathian Basin, is  
107 deficient or missing (Szigeti et al., 2015). The major objective of this study was to present, discuss and  
108 interpreted the OP data determined by AA and DTT assays in PM<sub>2.5</sub>-fraction aerosol samples collected in  
109 parallel in central Budapest, its suburban area and rural background within the Carpathian Basin in each  
110 season over one year. We also investigated the spatiotemporal dependencies, and identified the main  
111 aerosol sources of OP. The study can contribute to our general knowledge on the OP as well.

## 112 **2 Methods**

### 113 **2.1 Sample collections**

114 The samplings in the rural background were performed at the K-puszta station (N 46° 57' 56", E 19° 32'  
115 42", 125 m above sea level, a.s.l.), which represents the main plain part of the basin (Salma et al., 2020a).  
116 Budapest, with ca. 2.2 million inhabitants in the metropolitan area, is the largest city in the region. Its  
117 suburban environment was characterised by collections at the Marczell György Main Observatory (N 47°  
118 25' 46", E 19°10' 54", 138 m a.s.l.) of the Hungarian Meteorological Service (Salma et al., 2022). This is  
119 in a southeast residential part of the city. The samplings in the city centre were accomplished at the  
120 Budapest platform for Aerosol Research and Training (BpART) Laboratory (N 47° 28' 30", E 19° 03' 45",  
121 115 m a.s.l.), which represents an average atmosphere of the city centre (Salma et al., 2016).

122

123 Three identical high-volume sampling devices equipped with PM<sub>2.5</sub> inlets (DHA-80, Digitel, Switzerland)  
124 were deployed at the sites (Salma et al., 2020a). The collection substrates were prebaked quartz fibre  
125 filters with a diameter of 150 mm (QR-100, Advantec, Japan). Daily aerosol samples were taken starting  
126 at midnight of local time. The samples corresponding to air volumes of 720 m<sup>3</sup> were collected in parallel  
127 with each other over semi-consecutive days in October 2017 (autumn), January 2018 (winter), April 2018  
128 (spring) and July 2018 (summer). The total numbers of the filters were 56 in the rural background, 59 in  
129 the suburban area, and 28 in the city centre. The samples evenly spread among the four seasons. In  
130 addition, one field blank was taken at each location and in each season. The filters were wrapped in  
131 preheated Al foils, sealed in plastic bags and stored at a temperature of <-4 °C until the analyses. The

132 samples represent a gradual transition from the central part of a large continental European city through  
133 its suburban area to its regional background in all seasons.

## 134 **2.2 Analyses and data treatment**

135 Particulate matter mass was determined by gravimetry (Cubis MSA225S-000-DA, Sartorius, Germany,  
136 sensitivity of 10  $\mu\text{g}$ ). The blank-corrected PM mass data were above the limit of quantitation (LOQ),  
137 which was 1  $\mu\text{g m}^{-3}$  (Salma et al., 2020a).

138

139 Filter punches were analysed by thermal-optical transmission method using a laboratory OC/EC analyser  
140 (Sunset Laboratory, USA) adopting the EUSAAR-2 thermal protocol (Cavalli et al., 2010). All blank-  
141 corrected organic carbon (OC) and elemental carbon (EC) data were above the LOQ, which were 0.38  
142 and 0.04  $\mu\text{g m}^{-3}$ , respectively. Filter pieces were analysed for levoglucosan (LVG) by gas  
143 chromatography–mass spectrometry (Varian 4000, USA) after trimethylsilylation (Blumberger et al.,  
144 2019). All blank-corrected LVG data were above the LOQ, which was 1.2  $\text{ng m}^{-3}$ .

145

146 Parts of the filters were analysed by particle-induced X-ray emission spectrometry for S, Cl, K, Ca, Ti,  
147 V, Cr, Mn, Fe, Co, Ni, Cu, Zn, As, Br, Rb, Sr, Zr, Ba and Pb using an external beam of protons with an  
148 energy of 2.35 MeV and a current of 20 nA (Aljboor et al., 2022). The obtained spectra were evaluated  
149 by the GUPIXWIN program. The filters were treated as thin layer samples. For S, Cl, K, Ca, the self-  
150 absorption effects of quartz filters were corrected for (Chiari et al., 2018). The lung bioaccessibility was  
151 assessed in the present work by the total amounts of the chemical species as the first approximation.

152

153 Concentrations of EC and OC from fossil fuel combustion and from biomass burning (BB), namely  $\text{EC}_{\text{FF}}$   
154 and  $\text{OC}_{\text{FF}}$ ,  $\text{EC}_{\text{BB}}$  and  $\text{OC}_{\text{BB}}$ , respectively and of OC from biogenic sources ( $\text{OC}_{\text{BIO}}$ ) were previously  
155 estimated by a coupled radiocarbon-LVG marker method (Salma et al., 2020a). Secondary organic carbon  
156 (SOC) was also assessed previously using the EC tracer method for primary OC (Salma et al., 2022).  
157 These results were used as supplementary data in interpretations.

## 158 **2.3 Determination of oxidative potential**

159 Specified filter areas were extracted in a simulated human respiratory tract lining fluid solution composed  
160 of Gamble's solution with dipalmitoylphosphatidylcholine (DPPC; the major phospholipid of lung  
161 surfactant; Calas et al., 2017, 2018). The extractions were carried out by vortex agitation at 37 °C for 1  
162 h. The overall procedure represents conditions which are close to the respiratory system. Isoconcentration

163 extracts with  $10 \mu\text{g ml}^{-1}$  of PM mass were obtained for all samples to overcome possible nonlinear OP  
164 response of PM concentrations (Charrier and Anastasio, 2012; Calas et al., 2017).

165

166 The sample extracts were not filtered, so they contained insoluble chemical species including those with  
167 active surface area (Baumann et al., 2023). The OP was measured by two single-compound in vitro  
168 acellular assays, i.e. AA and DTT assays. These two methods are widely used for OP determination (e.g.  
169 Calas et al., 2018; Daellenbach et al., 2020; Lionetto et al., 2021; Shahpoury et al., 2021, 2022). However,  
170 there is a fundamental difference between them regarding their underlying chemical mechanisms  
171 (Charrier and Anastasio, 2012). The quantifications were based on plate-reader spectrophotometry (Tecan  
172 Infinite M200 Pro, Switzerland) in MilliQ water for AA, and in a phosphate buffer with a physiological  
173 pH value of 7.4 after adding 5,5'-dithiobis(2-nitrobenzoic acid), with readings taken at different specified  
174 reaction times (Calas et al., 2018; Borlaza et al., 2021b, 2022). The possible transition metal  
175 contamination of the buffer was removed by Chelex 100 resin to reduce the background oxidation. The  
176 consumption rates of the AA or DTT were obtained from the simple linear regression of the absorbance  
177 values in time at 265 and 412 nm, respectively. The coefficients of determination  $R^2$  for the regression  
178 were  $>0.90$  when  $<70\%$  of the initial amount of the reagent was oxidised. Matrix absorbance was  
179 considered, and the quality assurance of the determinations was performed by positive control tests  
180 (Borlaza et al., 2021b). The limits of detection (LODs) for the AA and DTT assays were set at three times  
181 the standard deviation (SD) for the blank extracts and were typically  $0.008$  and  $0.0014 \text{ nmol min}^{-1}$ ,  
182 respectively. The experimental protocols were described in more detail previously (Calas et al., 2017,  
183 2018).

184

185 The OP data measured by the AA and DTT assays were normalised to  $\text{PM}_{2.5}$  mass ( $m$ ) or sampled air  
186 volume ( $V$ ) and are denoted as  $\text{OP}_{\text{AA},m}$ ,  $\text{OP}_{\text{DTT},m}$ ,  $\text{OP}_{\text{AA},V}$  and  $\text{OP}_{\text{DTT},V}$ . The consumption rates normalized  
187 to  $V$  are often considered to have a closer relationship to human exposure, while those normalized by  $m$   
188 are regarded as a measure of the inherent OP of PM (Weber et al., 2018; Yu et al., 2019).

## 189 **2.4 Mathematical models**

190 Source apportionment modelling was accomplished to identify and quantify the main aerosol sources  
191 using positive matrix factorisation (PMF, US Environmental Protection Agency, version 5.0; EPA, 2017).  
192 It decomposes the sample data matrix into a linear combination of two matrices: a daily factor contribution  
193 varying in time and factor profiles by minimizing the critical compound parameter  $Q$  (Paatero and Tapper,  
194 1994; Hopke, 2016, 2000). The input data set contained the concentrations and uncertainties of  $\text{PM}_{2.5}$   
195 mass, S, Cl, K, Ca, Ti, V, Cr, Mn, Fe, Ni, Cu, Zn, Br, Rb, Ba, Pb, EC, OC and LVG for all sampling sites

196 and seasons. A multisite PMF modelling with 143 samples was performed (Dai et al., 2020). For most  
197 chemical species, all concentrations were higher than the LODs. For some trace elements, the  
198 concentrations were larger than the LODs in >60 % of the samples. The missing data were replaced by  
199 the related median with an uncertainty of 5/6 of the LOD value. The concentrations above LODs were  
200 associated with an equation-based extra standard deviation in accordance with the guidelines of the PMF  
201 manual, which involved the measurement uncertainty, the concentration and the LOD values (EPA,  
202 2017). Elements Cl, Cr, Ni and Rb were specified as weak variables due to their relatively large SDs.

203

204 Several test runs were performed with a total number of factors ranging from 3 to 9 to define the base  
205 runs. To explore the goodness of the individual results and to derive robust source apportionment,  
206 additional mathematical tools such as bootstrapping and displacement methods were adopted (Norris et  
207 al., 2014). In bootstrapping, the compliance between the base factors and bootstrapped factors (which  
208 were later selected as the final solution) was >80 %. In addition, the displacement for these solutions did  
209 not show larger changes in the parameter Q and no swap counts of factors occurred.

210

211 Multiple linear regression (MLR) modelling was performed to deconvolute the measured  $OP_{AA,V}$  and  
212  $OP_{DTT,V}$  data sets as the dependent variables among the main aerosol sources identified by the PMF as the  
213 independent variables (Weber et al., 2021). A linear predictor function was fitted through the dependent  
214 variable points by the weighted least squares (WLS) method. The weights were chosen as the inverse of  
215 the square of the SD for each measured OP. Goodness of the fit was checked by residual analysis. The  
216 significant predictor variables were selected using an *F*-test. The calculations were performed in the  
217 advanced analytics software package Statistica (version 7.1, StatSoft, Germany).

## 218 **3 Results and discussion**

### 219 **3.1 Ranges, averages and tendencies**

220 Basic statistics of the daily OP data and atmospheric concentrations obtained from the filters for the whole  
221 sampling interval in the three environments are summarised in Table 1. Some further atmospheric  
222 concentrations measured online and the local meteorological data together with their measuring methods  
223 are given in Sect. S1 in the Supplement. The concentrations of  $EC_{FF}$ ,  $OC_{FF}$ ,  $EC_{BB}$ ,  $OC_{BB}$ ,  $OC_{BIO}$  and SOC  
224 derived earlier can be found in previous publications (Salma et al. 2020a, 2022). The present average  
225 concentrations and meteorological data are in line with the results of earlier studies (Salma et al., 2004,  
226 2005, 2020a; Szigeti et al., 2015) suggesting that the overall data set represents typical atmospheric  
227 conditions at the locations. However, several Saharan dust intrusions into the Carpathian Basin happened

228 in April 2018 (Varga, 2020). The most intensive event reached the region via southern Italy and the  
 229 Balkans on 15 April and affected the studied region for a few days.

230

231 **Table 1.** Ranges and medians of oxidative potential (OP) determined by AA and DTT assays and normalised to PM mass ( $m$ ;  
 232  $OP_{AA,m}$  and  $OP_{DTT,m}$ , respectively, in unit of  $\text{nmol min}^{-1} \mu\text{g}^{-1}$ ) or to sampled air volume ( $V$ ;  $OP_{AA,V}$  and  $OP_{DTT,V}$ , respectively,  
 233  $\text{nmol min}^{-1} \text{m}^{-3}$ ), of concentrations for  $\text{PM}_{2.5}$  mass ( $\mu\text{g m}^{-3}$ ), chemical elements (all in  $\text{ng m}^{-3}$ ), elemental carbon (EC), organic  
 234 carbon (OC, both in  $\mu\text{g m}^{-3}$ ), levoglucosan (LVG,  $\text{ng m}^{-3}$ ) in the rural background, suburban area and city centre.

235

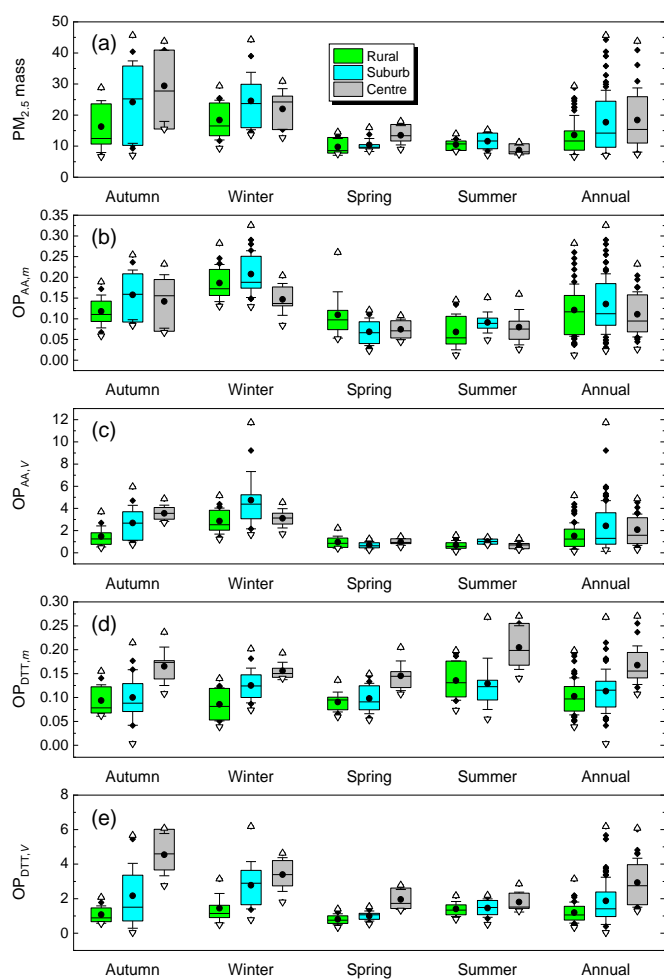
| Site/<br>Variable | Rural background |        |         | Suburban area |        |         | City centre |        |         |
|-------------------|------------------|--------|---------|---------------|--------|---------|-------------|--------|---------|
|                   | Minimum          | Median | Maximum | Minimum       | Median | Maximum | Minimum     | Median | Maximum |
| $OP_{AA,m}$       | 0.01             | 0.12   | 0.28    | 0.02          | 0.14   | 0.33    | 0.03        | 0.11   | 0.23    |
| $OP_{AA,V}$       | 0.1              | 1.5    | 5.2     | 0.3           | 2.4    | 11.7    | 0.3         | 2.1    | 4.9     |
| $OP_{DTT,m}$      | 0.04             | 0.10   | 0.20    | 0.004         | 0.11   | 0.27    | 0.11        | 0.17   | 0.27    |
| $OP_{DTT,V}$      | 0.3              | 1.2    | 3.1     | 0.03          | 1.9    | 6.2     | 1.3         | 2.9    | 6.1     |
| $\text{PM}_{2.5}$ | 6                | 14     | 29      | 7             | 18     | 46      | 7           | 18     | 44      |
| S                 | 51               | 311    | 1043    | 84            | 312    | 823     | 167         | 367    | 952     |
| Cl                | 5                | 11     | 28      | 5             | 32     | 118     | 5           | 23     | 71      |
| K                 | 11               | 56     | 234     | 9             | 65     | 363     | 18          | 91     | 264     |
| Ca                | 1                | 33     | 215     | 6             | 73     | 457     | 23          | 104    | 468     |
| Ti                | 0.05             | 1.3    | 15      | 0.3           | 1.9    | 26      | 0.6         | 3.1    | 22      |
| V                 | 0.23             | 0.46   | 1.1     | 0.13          | 0.43   | 1.0     | 0.13        | 0.44   | 1.2     |
| Cr                | 0.16             | 0.37   | 0.91    | 0.18          | 0.46   | 1.7     | 0.17        | 0.76   | 7.2     |
| Mn                | 0.4              | 2.0    | 16      | 0.1           | 2.1    | 5.6     | 0.5         | 3.3    | 11      |
| Fe                | 5                | 32     | 162     | 16            | 63     | 306     | 33          | 102    | 607     |
| Ni                | 0.13             | 0.42   | 1.3     | 0.14          | 0.33   | 1.1     | 0.18        | 0.57   | 3.0     |
| Cu                | 0.13             | 0.94   | 6.8     | 0.6           | 1.6    | 7.5     | 0.8         | 2.9    | 27      |
| Zn                | 0.9              | 7.2    | 40      | 3             | 12     | 53      | 1           | 17     | 48      |
| Br                | 0.20             | 0.77   | 3.0     | 0.2           | 1.2    | 4.1     | 0.5         | 1.3    | 2.7     |
| Rb                | 0.22             | 0.35   | 0.76    | 0.22          | 0.36   | 0.83    | 0.24        | 0.34   | 0.80    |
| Ba                | 1.1              | 2.4    | 12      | 1.1           | 3.1    | 12      | 1.1         | 4.5    | 13      |
| Pb                | 0.6              | 3.4    | 28      | 1.5           | 5.3    | 21      | 1.3         | 5.6    | 19      |
| EC                | 0.08             | 0.22   | 0.77    | 0.21          | 0.50   | 1.1     | 0.31        | 0.78   | 1.8     |
| OC                | 0.9              | 2.3    | 6.0     | 1.0           | 2.9    | 11      | 2.0         | 3.3    | 8.0     |
| LVG               | 4                | 38     | 776     | 5             | 106    | 1765    | 8           | 203    | 709     |

236

237 The average  $\text{PM}_{2.5}$  mass,  $OP_{AA}$  and  $OP_{DTT}$  data sets showed three different tendencies with respect to the  
 238 locations. This is better visualised with their annual mean and median data in Fig. 1. The averages (i.e.  
 239 the medians and means) of the  $\text{PM}_{2.5}$  mass exhibited a rising trend with levelling off from the rural  
 240 background through the suburban area to the city centre. The means of both  $OP_{AA,m}$  and  $OP_{AA,V}$  data sets  
 241 indicated a maximum in the suburban background, whereas the tendencies for their medians were not  
 242 fully conclusive. The differences in the tendencies already suggest that there is a misalignment between  
 243 the PM mass and the OP data and that the two assays used show different sensitivity to source types active  
 244 at the locations.



245  
 246  
 247  
 248  
 249  
 250  
 251  
 252  
 253  
 254  
 255  
 256  
 257  
 258  
 259  
 260  
 261  
 262  
 263  
 264  
 265  
 266  
 267  
 268  
 269  
 270  
 271  
 272  
 273



274 **Figure 1.** Box and whisker plots of  $\text{PM}_{2.5}$  mass concentration ( $\mu\text{g m}^{-3}$ ; panel a), oxidative potential (OP) determined by AA  
 275 and DTT assays and normalised to PM mass ( $m$ ;  $\text{OP}_{\text{AA},m}$  and  $\text{OP}_{\text{DTT},m}$ ,  $\text{nmol min}^{-1} \mu\text{g}^{-1}$ ; panels b and d) or to sampled air  
 276 volume ( $V$ ;  $\text{OP}_{\text{AA},V}$  and  $\text{OP}_{\text{DTT},V}$ ,  $\text{nmol min}^{-1} \text{m}^{-3}$ ; panels c and e) in the rural background, suburban area and city centre  
 277 separately for each season and over one year. Maximum and minimum values (triangles pointing upward and downward,  
 278 respectively), further extreme values (diamonds), the first and third quartiles (lower and upper horizontal borders of the boxes,  
 279 respectively), median (horizontal line inside the boxes), means (bullets) and  $\pm 1$  SDs (whiskers) of the data sets are shown.  
 280

281 Basic statistics of  $\text{PM}_{2.5}$  mass and OP data separately for each season and the whole year are shown in  
 282 Fig. 1. In winter and autumn (the heating period), the OP and PM mass levels were higher than in spring  
 283 and summer. This is consistent with the other continental European sites (e.g. Calas et al., 2019; Borlaza  
 284 et al., 2022). The heating period-to-non-heating period OP ratios in the urban locations were larger than  
 285 for the rural background by factors of ca. 4 for  $\text{OP}_{\text{AA},V}$  and 1–2 for  $\text{OP}_{\text{DTT},V}$ . There were similar tendencies  
 286 in the OP values derived by both AA and DTT assays over the seasons. Except for the  $\text{OP}_{\text{DTT},m}$  data,  
 287 which showed a fairly constant level over the seasons with some higher values in summer, particularly in

288 the city centre. This can be again linked to the altered chemical composition of PM mass in time and to  
289 the different responses of the two assays to this change.

290

291 There are only a few other OP data sets for the PM<sub>2.5</sub> size fraction derived by AA and DTT assays. Their  
292 comparison to our OP data is hindered by important experimental details such as the extracted amount of  
293 PM from filters. It can be identified that our median OP values are larger than those at other European  
294 sites (Daellenbach et al., 2020; Grange et al., 2022, In 't Veld et al., 2023), while they belong to the middle  
295 range of the available results for Japan and China (Kurihara et al., 2022; Yu et al., 2019). The differences  
296 can be also influenced by the exact location type since higher OP data near traffic sources were observed  
297 (Boogaard et al., 2012; Fang et al., 2016; Daellenbach et al., 2020).

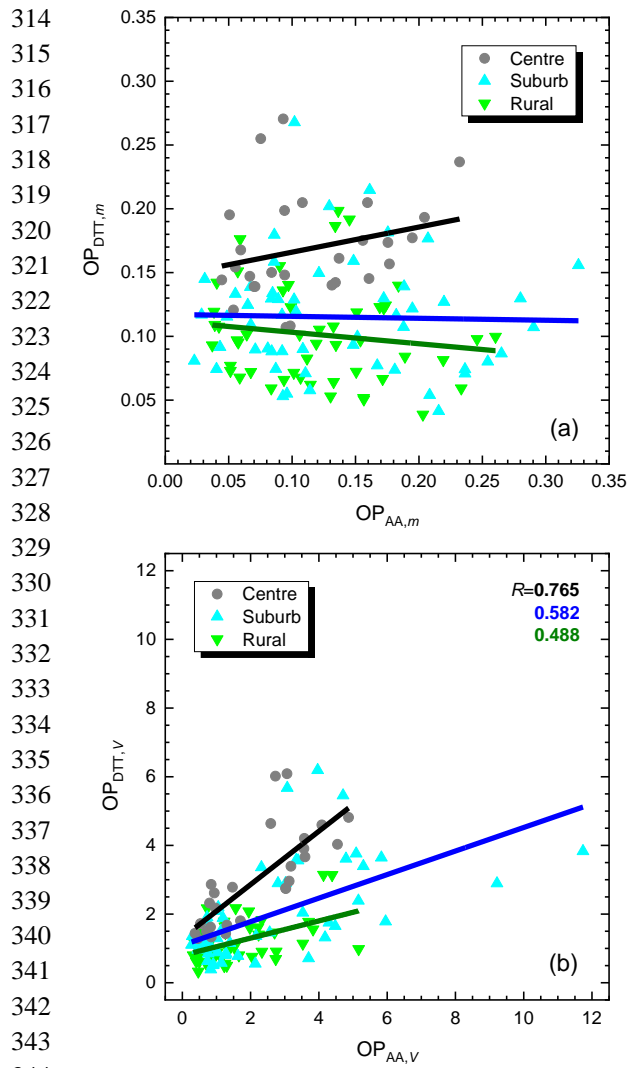
### 298 **3.2 Consistency between the assays**

299 The dependencies between the OP data derived by the AA assay and normalised either to  $m$  or  $V$  on the  
300 corresponding DTT data are displayed in Fig. 2. Pearson's coefficients of correlation ( $R$ ) between the data  
301 sets normalised to  $m$  (Fig. 2a) were not significant ( $p=0.05$ ) at the locations. It suggests that the OP <sub>$m$</sub>  was  
302 controlled by chemical species that invoked different responses in the assays. However, all correlations  
303 between the two OP data sets normalised to  $V$  (Fig. 2b) were significant. The slopes with SDs of the  
304 regression lines were smaller than unity ( $0.25\pm 0.06$ ,  $0.34\pm 0.07$  and  $0.78\pm 0.13$ , respectively) and increased  
305 monotonically from the rural background through the suburban area to the city centre.

306

307 The results suggested that the OP<sub>DTT</sub> and OP<sub>AA</sub> values normalised to sampled air volume were in line and  
308 consistent. The slopes of their regression lines (Fig. 2b) were  $<1$ , which is interpreted as that the AA assay  
309 reacted more sensitively to the changes in chemical composition of PM than the DTT assay at our  
310 locations. More importantly, the conclusions underline the need for deploying multiple (at least two) OP  
311 assays, particularly in cleaner atmospheric environments, to achieve a more holistic and consistent picture  
312 (Calas et al., 2017; Bates et al., 2019; Borlaza et al., 2022; Shahpoury et al., 2022).

313



345 **Figure 2.** Scatter plots of the oxidative potential (OP) values determined by AA and DTT assays and normalised to PM mass  
 346 ( $m$ ;  $OP_{AA,m}$  and  $OP_{DTT,m}$ , in  $\text{nmol min}^{-1} \mu\text{g}^{-1}$ ; panel a) or to sampled air volume ( $V$ ;  $OP_{AA,V}$  and  $OP_{DTT,V}$ ,  $\text{nmol min}^{-1} \text{m}^{-3}$ ; panel  
 347 b) separately in the rural background, suburban area and city centre. The coefficients of correlation ( $R$ s) for the significant  
 348 cases are also given.

### 349 3.3 Main aerosol sources

350 Six factors resolved by the PMF modelling were further evaluated as described in Sect. S2. The following  
 351 aerosol sources were identified: biomass burning, suspended dust, road traffic, oil combustion mixed with  
 352 coal combustion and particularly, with long-range transport in the rural background during the nonheating  
 353 period (Sect. S2), vehicle metal wear and mixed industrial source. Similar set of source types was also  
 354 identified earlier for Budapest in larger number of samples in winter (Furu et al., 2022).

355

356 The apportionments of the  $\text{PM}_{2.5}$  mass among the main sources are summarised in Fig. 3 separately for  
 357 each location and season. The plots reveal that the source contributions changed very substantially over  
 358 the year.

359

360

361

362

363

364

365

366

367

368

369

370

371

372

373

374

375

376

377

378

379

380

381

382

383

384

385

386

387

388

389

390

391

392

393

394

395

396

397

398

399

400

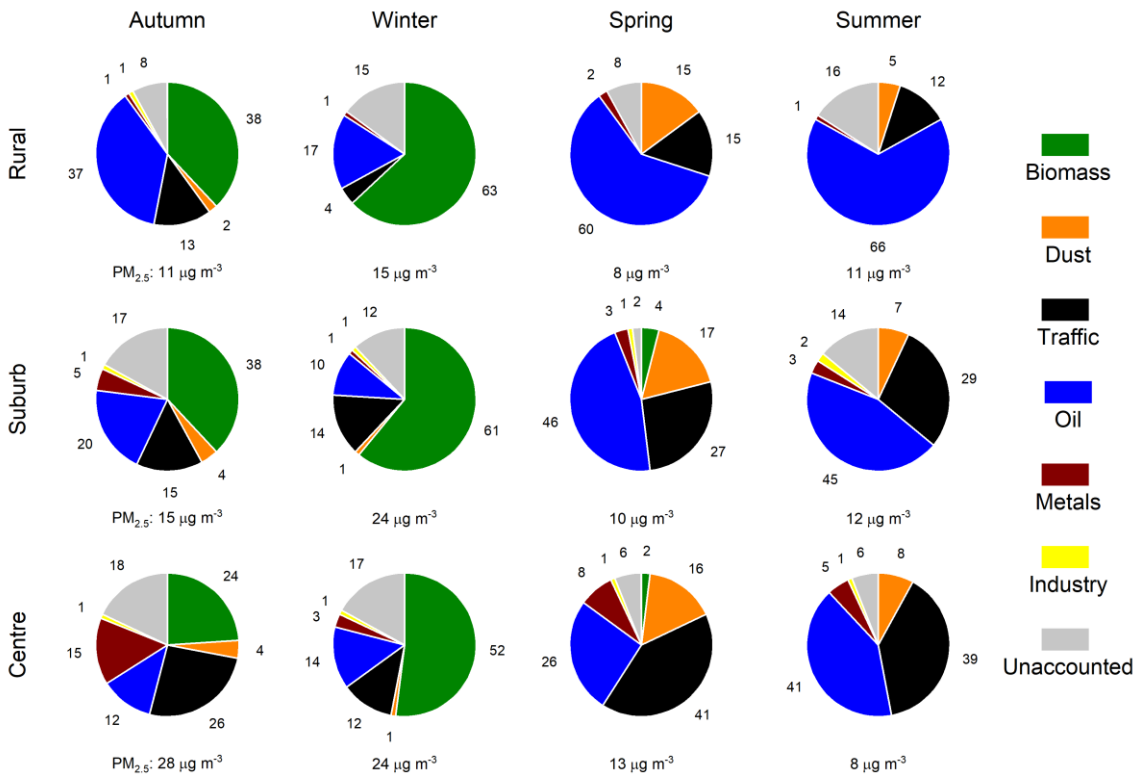


**Figure 3.** Mean contributions of biomass burning, suspended dust, road traffic, oil combustion mixed with coal combustion and long-range transport, vehicle metal wear, mixed industrial source and unaccounted sources to the atmospheric concentration of PM<sub>2.5</sub> mass (in %) as derived by the PMF modelling in the rural background, suburban area and city centre in different seasons. The median atmospheric concentrations are shown under the circle charts.

387

388

389

390

391

392

393

394

395

396

397

398

399

400

In winter, BB was the dominant source (with mean contributions of 50 % – 60 %) at all sites. In autumn, BB and oil combustion mixed with coal combustion and long-range transport were the two most important sources in the rural background with similar shares (38 %). In the suburban area, BB exhibited very similar (38 %) contribution to the rural background, whereas oil combustion and the joint importance of road traffic and vehicle metal wear showed the second largest and similar contributions (20 %). In the city centre, traffic-related sources were the most important contributors (40 %). In spring, oil combustion prevailed (60 %) in the rural background. Its contribution monotonically decreased through the suburban area (46 %) to the city centre (26 %). In parallel with this tendency, the joint share from road traffic and vehicle metal wear increased monotonically (from 17 % through 30 % to 49 %) in the same order of the locations. The contributions from suspended dust in spring were also significant at all locations accounting for approximately 15%. They were influenced by the Saharan dust intrusion episodes extending over the whole Carpathian Basin in this season. In summer, oil combustion was again the dominant source (66 %) in the rural background and showed a decreasing share for the suburban area (45

401 %) to the city centre (41 %). Contrary, the effects of road traffic monotonically rose (from 13 % through  
402 31 % to 44 %). This increasing tendency was preserved in the other seasons as well. The unaccounted  
403 sources and their possible effects on the final results are discussed in Sect. 3.6.

404

405 The apportionments of Cu and Fe, which are of special interest for OP, among the main aerosol sources  
406 as derived by the PMF modelling are shown in Figs. S7 and S8. Copper mainly or dominantly originated  
407 from motor vehicles, i.e. vehicle metal wear and road traffic sources except for the rural background in  
408 winter and autumn. The outstanding role of road vehicles is confirmed by our earlier results for a street  
409 canyon in central Budapest (Salma and Maenhaut, 2006). The smallest shares from vehicles occurred in  
410 winter (22 %, 39 % and 65 %, respectively in the rural background, suburban area and city centre), while  
411 the maximum contributions happened in summer (51 %, 65 % and 87 %, respectively). The contribution  
412 of unaccounted sources in the rural background in winter was large (33 %), which could modify the  
413 apportionments. The role of BB in Cu emissions could be possible explained by illegal industrial and  
414 household waste burnings together with biomass (Sect. S2; Hoffer et al., 2021).

415

416 In the city centre, the vehicle sources showed the largest contributions to Fe (53 % – 74 %) in all seasons,  
417 and dust was its second most intensive source (30 %–36 %) in spring and summer. At the other two  
418 locations, Fe in spring was unambiguously dominated by dust (ca. 55 %), which was influenced by the  
419 Saharan dust intrusion. Suspended dust remained the most important source in the rural background in  
420 summer, whereas it became comparable to the traffic-related sources in the suburban area. Vehicles  
421 tended to be the second largest Fe source (26 % – 45 %) in the rural background and suburban area. Their  
422 contributions could be partly also associated with the resuspended road dust generated by moving  
423 vehicles. In autumn, the shares in the rural background were more or less balanced among the main  
424 sources, while the vehicle contributions were increased in the suburban area.

425

426 The examples of Cu and Fe demonstrated broadly varying spatial and temporal tendencies in the source  
427 contributions of OP-active chemical species and point to the potentials of regulatory measures based on  
428 specifically selected source types.

### 429 **3.4 Oxidative potential and aerosol sources**

430 The OP data normalised to sampled air volume were apportioned to the main aerosol sources, i.e. of BB,  
431 suspended dust, road traffic, oil combustion mixed with coal combustion and long-range transport, vehicle  
432 metal wear and mixed industrial source using the MLR method with the WLS approach. The slopes and  
433 intercepts of the regression lines calculated for the whole data set at each sampling location are

434 summarised in Table S4. In a few cases, negative slopes were obtained. This is commonly found with this  
 435 approach, but the absolute values of the negative slopes should be relatively small. This was not the case  
 436 for the vehicle metal wear and  $OP_{DTT,V}$  pair in the rural background, for the road traffic and  $OP_{AA,V}$  pair  
 437 in the suburban area, and for the oil combustion and  $OP_{AA,V}$  pair in the city centre. The intercepts of the  
 438  $OP_{DTT,V}$  in the suburban area and city centre also resulted in statistically nonzero values. These cases  
 439 jointly indicate that there could be some aerosol sources missing in the PMF modelling due probably to  
 440 the unavailability of some important marker variables and to the limited number of samples. The  
 441 shortcoming is further discussed in Sect. 3.6. It cannot be excluded that this imperfection influences the  
 442 order and mainly the contributions of the OP sources. To improve the attribution of the OP to the identified  
 443 aerosol sources, the MLR model with the WLS approach was also performed with forced positive slopes  
 444 option. Its constrained results are summarised in Table 2.

445

446 **Table 2.** Slopes and intercepts of the multiple linear regression with the weighted least squares approach and forced positive  
 447 slopes option between oxidative potential (OP) determined by AA and DTT assays and normalised to sampled air volume  
 448 ( $OP_{AA,V}$  and  $OP_{DTT,V}$ , respectively; in  $\text{nmol min}^{-1} \text{m}^{-3}$ ) and the main aerosol sources of biomass burning, suspended dust, road  
 449 traffic, oil combustion mixed with coal combustion and long-range transport, vehicle metal wear and mixed industrial source  
 450 derived by PMF modelling in the rural background, suburban area and city centre. The number of samples available ( $n$ ) and  
 451 the adjusted coefficients of determination ( $R^2$ ) are also shown. Nonsignificant values are in *Italic* font.

452

| Location/<br>Main source | Rural background |              | Suburban area |               | City centre   |               |
|--------------------------|------------------|--------------|---------------|---------------|---------------|---------------|
|                          | $OP_{AA,V}$      | $OP_{DTT,V}$ | $OP_{AA,V}$   | $OP_{DTT,V}$  | $OP_{AA,V}$   | $OP_{DTT,V}$  |
| Biomass burning          | 1.414            | 0.873        | 0.792         | 0.622         | 1.073         | 0.788         |
| Suspended dust           | <i>0.113</i>     | –            | 0.569         | <i>0.018</i>  | <i>0.025</i>  | <i>0.090</i>  |
| Road traffic             | 1.010            | 0.959        | –             | <i>0.181</i>  | 0.357         | 0.887         |
| Oil combustion           | 0.279            | –            | <i>0.522</i>  | 0.968         | –             | <i>0.488</i>  |
| Vehicle metal wear       | <i>0.056</i>     | –            | –             | –             | <i>0.018</i>  | <i>0.091</i>  |
| Mixed industrial         | –                | <i>0.085</i> | <i>0.172</i>  | <i>0.086</i>  | <i>0.142</i>  | –             |
| Intercept                | <i>–0.160</i>    | <i>0.358</i> | <i>–0.473</i> | <i>–0.497</i> | <i>–0.081</i> | <i>–0.362</i> |
| $n$                      | 52               | 51           | 56            | 55            | 28            | 28            |
| $R^2$                    | 0.974            | 0.877        | 0.717         | 0.779         | 0.858         | 0.811         |

453

454 With this latter option, all intercepts became statistically insignificant ( $p < 0.05$ ) from zero. The AA assay  
 455 yielded significant slopes with BB, road traffic and oil combustion in the rural background, with BB and  
 456 suspended dust in the suburban area and with BB, and road traffic in the city centre. The DTT assay  
 457 resulted in significant slopes with BB and road traffic, with BB and oil combustions and with BB and  
 458 road traffic in the three environments. Comparing the fitted MLR parameters obtained by the constrained  
 459 and non-constrained WLS approaches (Tables 2 and S4) shows that the orders of the sources did not

460 change substantially, and that the positive slopes obtained by the two models are comparable. At the same  
461 time, the importance of oil combustion decreased in some occasions. These likely indicate that the derived  
462 ranks of the OP sources are sensible approximations to reality with some larger uncertainties of their  
463 contributions.

464

465 The driving effect of BB on OP has been highlighted in other studies (e.g. Verma et al., 2015; Lionetto et  
466 al., 2021; Borlaza et al., 2022). The intensity of BB in the Carpathian Basin is, however, large only in the  
467 heating period (autumn and winter), and much lower outside this interval. To refine the apportionment of  
468 the OP data to aerosol sources active in the non-heating seasons, the MLR modelling was repeated with  
469 the joint data set of all sites split into heating and non-heating periods. These results confirmed that BB  
470 shows overwhelming contributions to the OP values in the heating period independently of the intensity  
471 of the vehicle road traffic. The latter changed substantially among the rural background and urban sites.  
472 More importantly, the obtained results also imply that the shares from vehicles (i.e. joint sources of road  
473 traffic and vehicle metal wear) to OP prevailed in the non-heating period. This is in line with the  
474 attributions of some transition metals such as Cu and Fe to these aerosol sources (Figs. S7–S8 and Salma  
475 and Maenhaut, 2006), and also points to the remarkable role of primary traffic emissions in causing  
476 oxidative stress in spring and summer.

477

478 Secondary organic aerosol under anthropogenically influenced conditions was proven to be one of the top  
479 factors for OP (Srivastava et al., 2018; Wong et al., 2019; Daellenbach et al., 2020; Borlaza et al., 2021a,  
480 2021b; Pye et al., 2021; Zhang et al., 2022). The involvement of the SOC concentrations into the PMF  
481 was hampered by their smaller count and larger relative uncertainty (up to 30 % – 50 %; Salma et al.,  
482 2022). Instead, we investigated the correlations between the OP data sets and SOC concentrations or  
483 SOC/OC ratios. The dependencies of the  $OP_{DTT,V}$  on the SOC are shown in Fig. S9. The OP values at the  
484 urban locations tended to increase with the SOC in parallel with each other, while the OP was rising in a  
485 smaller rate in the regional background. The reasons behind these observations likely include the distinct  
486 effects of biogenic and anthropogenic secondary organic aerosols typically present in different portions  
487 at the sampling locations. The results may indirectly indicate that photochemical aging processes and  
488 SOC formation over seasons impact the OP of PM as well (Wong et al., 2019; Kodros et al., 2020; Zhang  
489 et al., 2022). The increasing slope of the regression lines from the rural background to the city centre  
490 shown in Fig. 2b may also imply that organics of biogenic origin exhibit smaller responses in the DTT  
491 assays than those of BB (Verma et al., 2015) or of urban sources in general. There were no significant  
492 correlations obtained for the other data pairs.

### 493 3.5 Oxidative potential and air quality

494 Particulate matter mass was proven to be the most important component from the criteria air pollutants in  
495 the Carpathian Basin (Salma et al., 2020a, 2020b). Generally, this measure expresses the air quality in the  
496 basin. Therefore, the relationships between the  $PM_{2.5}$  mass and OP data sets normalised to sampled air  
497 volume were separately investigated. Their correlation dependencies were all significant (Fig. 4). Spatial  
498 and temporal correlations between these variables from low to moderate were also observed in earlier  
499 studies under broadly varying conditions (Künzli et al., 2006; Boogaard et al., 2012; Yang et al., 2015;  
500 Fang et al., 2016; Chirizzi et al., 2017).

501

502

503

504

505

506

507

508

509

510

511

512

513

514

515

516

517

518

519

520

521

522

523

524

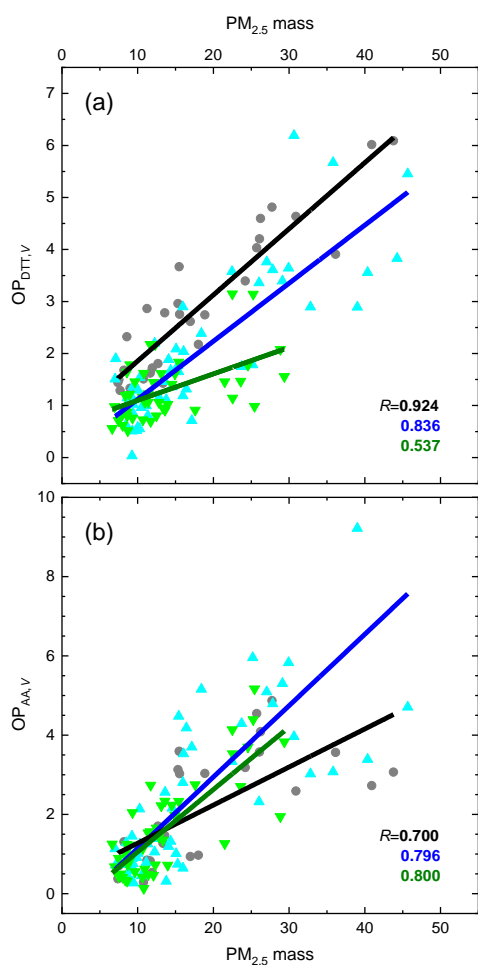
525

526

527

528

529



530 **Figure 4.** Scatter plots of the oxidative potential (OP) determined by DTT (a) and AA (b) assays and normalised to sampled  
531 air volume ( $V$ ;  $OP_{DTT,V}$  and  $OP_{AA,V}$ , respectively, in  $\text{nmol min}^{-1} \text{m}^{-3}$ ) and  $PM_{2.5}$  mass concentrations ( $\mu\text{g m}^{-3}$ ) for the rural  
532 background, suburban area and city centre. The lines represent linear regressions of the data sets. The coefficients of correlation  
533 ( $R$ s) are also indicated.

534

535 The dependencies for the  $OP_{DTT,V}$  (Fig. 4a) resulted in two almost parallel lines (with slopes and SDs of  
536  $0.11 \pm 0.01$  and  $0.13 \pm 0.01 \text{ nmol min}^{-1} \mu\text{g}^{-1}$ , respectively) in the city centre and suburban area, while a



537 smaller slope ( $0.051\pm 0.012 \text{ nmol min}^{-1} \mu\text{g}^{-1}$ ) was observed in the rural background. The situation for the  
538  $\text{OP}_{\text{AA,V}}$  (Fig. 4b) was less obvious but somewhat similar to  $\text{OP}_{\text{DTT,V}}$ . The regression lines for the rural  
539 background and suburban area tended to be fairly parallel with each other (with slopes and SDs of  
540  $0.16\pm 0.02$  and  $0.18\pm 0.02 \text{ nmol min}^{-1} \mu\text{g}^{-1}$ , respectively), whereas the slope for the city centre was smaller  
541 ( $0.096\pm 0.019 \text{ nmol min}^{-1} \mu\text{g}^{-1}$ ). The intercepts could be typically regarded to be zero within the  
542 uncertainty interval.

543

544 The parallel tendencies may indicate that the effects of the PM chemical compositions on the given assay  
545 were close to each other at the sampling locations with the parallel lines. This was likely caused by spatial  
546 and temporal similarities in the main sources such as road traffic and resuspended dust particularly for  
547 the DTT assay, and biomass burning especially for the AA assay (Salma et al., 2020a). Particles in the  
548 third environment (with the smaller slope) likely contained less OP-active components from the point of  
549 the given assay and, therefore, the increase in the OP was more modest. This interpretation is confirmed  
550 by earlier similar conclusions (Daellenbach et al., 2020). Nevertheless, it should be stressed that all slopes  
551 were substantially and much smaller than unity. This implies that the air quality regulatory measures  
552 based on the  $\text{PM}_{2.5}$  mass are expected to result in smaller improvements in oxidative stress compared to  
553 dedicated measures that specifically target (appropriately selected) aerosol sources.

### 554 **3.6 Limitations and later possibilities**

555 The total numbers of the samples collected at each location represent a limitation mainly for the PMF  
556 modelling. To overcome this problem, we applied multisite PMF. It was implicitly assumed in this  
557 approach that the main sources active at the locations can be characterised by similar chemical profiles.  
558 This is not completely fulfilled for all seasons. An example is the suspended dust which is virtually  
559 fugitive mineral and soil dust made of geogenic elements in the rural backgrounds. In the urban sites, it  
560 contains further constituents originally generated by anthropogenic activities, which settled down to  
561 surfaces and later entered into the air again by resuspension. It is mentioned that the PMF modelling on  
562 the separate locations yielded fairly similar results to the multisite approach, while the statistical  
563 uncertainties of these latter calculations were favourable.

564

565 The unavailability of some secondary inorganics, mainly nitrate and ammonium ions in the present  
566 analytical data sets introduced another limitation. Their contributions were likely contained in the  
567 unaccounted sources of the PMF modelling. They ranged up to 18 % and showed contributions mainly in  
568 colder (heating) seasons or in summer for the rural background and suburban area. Fortunately, pure  
569 secondary inorganic constituents are associated with lower contribution to OP of PM (Casseo et al., 2013;

570 Daellenbach et al., 2020), although they can influence the OP through acid mediated dissolution of  
571 transition metals (Fang et al., 2017). However, the robustness of the PMF modelling can influence the  
572 final apportion of the OP among the resolved sources.

573

574 Larger number of samples and extended list of variables are required because of the basin character of  
575 the region of interest. The poorest air quality in the whole Carpathian Basin generally occurs in winter  
576 (Salma et al., 2022), when persistent anticyclonic weather situations and lasting temperature inversions  
577 happen for longer times. During these intervals, the time series of aerosol constituents, even of different  
578 origins, change coherently at many locations due to the common effects of regional meteorology. This  
579 dependency can further encumber the separation of the aerosol sources in PMF modelling (Salma et al.,  
580 2004).

581

582 The present results and conclusions for the OP are strictly valid for the concrete sample preparation and  
583 selected assays. A more holistic picture can be achieved by deploying additional and extended  
584 experimental methods including those for the sample extraction treatment and OP measurement  
585 comprising advantageously both cellular and possibly further acellular assays. The present outcomes can  
586 be also improved by involving additional important chemical species and markers, mainly water-soluble  
587 metal ions, water-soluble OC, primary biogenic OC and PAHs. Extended research is required to address  
588 some additional relevant sources such as coal combustion, biogenic emissions and illegal waste burning.  
589 Investigations of size-fractionated aerosol samples with several toxicity indicators and possible synergism  
590 or antagonism among chemical species could bring further insights into the oxidative stress research. The  
591 experience gained in the present work, which was conducted in a systematic manner for the first time in  
592 this region, can form valuable experience in planning further related studies.

#### 593 **4 Conclusions**

594 We showed that the OP induced by PM<sub>2.5</sub> mass and determined by the AA and DTT assays in the rural  
595 (regional) background of the Carpathian Basin, in the suburban area and centre of its largest city of  
596 Budapest differed substantially and in a complex manner with location and changed considerably and  
597 consistently with season. The alterations were mainly caused by varying intensities of the main aerosol  
598 sources and possibly by other specific seasonal features. Biomass burning clearly exhibited the dominant  
599 influence at all locations in the heating period. Several pieces of indirect evidence suggest that the joint  
600 effects of motor vehicles involving road traffic and vehicle metal wear played the most important role in  
601 summer and spring, with considerable contributions from oil combustion and resuspended dust.

602

603 The most severe daily PM health limit exceedances in Budapest (and several other European cities) occur  
604 in winter due to both residential heating and meteorological effects. The contributions of BB to OP are  
605 the largest during this season. Thus, human exposure to high pollution levels are further exacerbated by  
606 the chemical composition which causes increased oxidative stress. As far as the sources related to motor  
607 vehicles are concerned, large traffic intensities frequently occur in city centres, which generate dangerous  
608 hotspots of particularly OP-active species. In these sites, an enhanced exposure of public in summer and  
609 spring often coincides with high population densities.

610

611 Our conclusions imply that targeting the PM mass in general does not efficiently reduce the oxidative  
612 burden from PM exposure. Instead, substantial health improvements could be achieved by focusing on  
613 some specific source types such as BB in winter and vehicle traffic in non-heating period. The former  
614 source may have timely consequences since it is expected to be increased in the near future. The non-  
615 exhaust emissions from vehicle traffic are anticipated to gain in relevance as well since high-efficiency  
616 exhaust gas aftertreatment devices had been already adopted to internal combustion engines and because  
617 of global spreading of electric vehicles. The advantages of BB and electric cars are often emphasized,  
618 while their potential drawbacks have been less disseminated. It is needed to further investigate their  
619 distinctive health effects for setting up effective mitigation policies and season-specific regulations.

620 *Data availability.* The observational data are available from the corresponding author.

621 *Supplement.* The supplement related to this article is available online at: *to be completed.*

622 *Author contributions.* MV evaluated the data, performed the modelling calculations, prepared figures, participated in  
623 interpreting the results and contributed to writing the manuscript; GU and J-LJ managed the OP measurements, GU, J-LJ and  
624 PD participated in interpreting the results and revising the manuscript; ZsK and EP managed the PIXE measurements and  
625 participated in interpreting the PMF results; IS conceived the research, arranged the sample collections, evaluated and  
626 interpreted the results, prepared figures, wrote the manuscript. All coauthors reviewed and commented on the manuscript.

627 *Competing interests.* The authors declare that they have no conflict of interest.

628 *Acknowledgements.* The authors are grateful to Anikó Angyal of the Institute for Nuclear Research for the PIXE measurements,  
629 to Attila Machon of the Hungarian Meteorological Service for the assistance in the sample collections and the OC/EC  
630 measurements, and to Anikó Vasanits of the Eötvös Loránd University for the LVG measurements.

631 *Financial support.* This research has been supported by the Hungarian Research, Development and Innovation Office (grants  
632 K132254 and K146915), the European Regional Development Fund and the Hungarian Government (grant GINOP-2.3.3-15-  
633 2016-00005) and the New National Excellence Program of the Ministry for Innovation and Technology from the source of the  
634 Hungarian Research, Development and Innovation Fund (ÚNKP-21-3). The OP analysis was supported by the ACME program  
635 (ANR-15-IDEX-02) and ANR Get OP Stand OP program (ANR-19-CE34-0002-01), and were analysed at the Air-O-Sol  
636 facility at IGE, made possible with the funding of some laboratory equipment by the Labex OSUG@2020 (ANR10 LABX56).

637 **References**

- 638 Abrams, J. Y., Weber, R. J., Klein, M., Samat, S. E., Chang, H. H., Strickland, M. J., Verma, V., Fang, T., Bates, J. T.,  
639 Mulholland, J. A., Russell, A. G., and Tolbert, P. E.: Associations between ambient fine particulate oxidative potential  
640 and cardiorespiratory emergency department visits, *Environ. Health Perspect.*, 125, 107008,  
641 <https://doi.org/10.1289/EHP1545>, 2017.
- 642 Aljboor, S., Angyal, A., Baranyai, D., Kertész, Zs., Papp, E., Szarka, M., Szikszai, Z., Rajta, I., and Vajda, I.: Light element  
643 sensitive in-air millibeam-PIXE setup for fast measurement of atmospheric aerosol samples, *J. Anal. At. Spectrom.*,  
644 submitted in 2022.
- 645 Apte, J. S., Marshall, J. D., Cohen, A. J., and Brauer, M.: Addressing global mortality from ambient PM<sub>2.5</sub>, *Environ. Sci.*  
646 *Technol.*, 49, 8057–8066, <https://doi.org/10.1021/acs.est.5b01236>, 2015.
- 647 Ayres, J. G., Borm, P., Cassee, F. R., Castranova, V., Donaldson, K., Ghio, A., Harrison, R. M., Hider, R., Kelly, F., Kooter,  
648 I. M., Marano, F., Maynard, R. L., Mudway, I., Nel, A., Sioutas, C., Smith, S., Baeza-Squiban, A., Cho, A., Duggan, S.,  
649 and Froines, J.: Evaluating the toxicity of airborne particulate matter and nanoparticles by measuring oxidative stress  
650 potential— a workshop report and consensus statement, *Inhal. Toxicol.* 20, 75–99,  
651 <https://doi.org/10.1080/08958370701665517>, 2008.
- 652 Baumann, K., Wietzoreck, M., Shahpoury, P., Filippi, A., Hildmann, S., Lelieveld, S., Berkemeier, T., Tong, H., and  
653 Lammel, G.: Is the oxidative potential of components of fine particulate matter surface-mediated?, *Environ. Sci. Pollut.*  
654 *Res.*, 30, 16749–16755, <https://doi.org/10.1007/s11356-022-24897-3>, 2023.
- 655 Bates, J. T., Weber, R. J., Abrams, J., Verma, V., Fang, T., Klein, M., Strickland, M. J., Sarnat, S. E., Chang, H. H.,  
656 Mulholland, J. A., Tolbert, P. E., and Russell, A. G.: Reactive oxygen species generation linked to sources of  
657 atmospheric particulate matter and cardiorespiratory effects, *Environ. Sci. Technol.*, 49, 13605–13612,  
658 <https://doi.org/10.1021/acs.est.5b02967>, 2015.
- 659 Bates, J. T., Fang, T., Verma, V., Zeng, L., Weber, R. J., Tolbert, P. E., Abrams, J. Y., Sarnat, S. E., Klein, M., Mulholland,  
660 J. A., and Russell, A. G.: Review of acellular assays of ambient particulate matter oxidative potential: methods and  
661 relationships with composition, sources, and health effects, *Environ. Sci. Technol.*, 53, 4003–4019,  
662 <https://doi.org/10.1021/acs.est.8b03430>, 2019.
- 663 Blumberger, Z. I., Vasanits-Zsigrai, A., Farkas, G., and Salma, I.: Mass size distribution of major monosaccharide  
664 anhydrides and mass contribution of biomass burning, <https://doi.org/10.1016/j.atmosres.2019.01.001>, *Atmos. Res.*,  
665 220, 1–9, 2019.
- 666 Boogaard, H., Janssen, N. A. H., Fischer, P. H., Kos, G. P. A., Weijers, E. P., Cassee, F. R., van der Zee, S. C., de Hartog, J.  
667 J., Brunekreef, B., and Hoek G.: Contrasts in oxidative potential and other particulate matter characteristics collected  
668 near major streets and background locations, *Environ. Health Perspect.*, 120, 2, <https://doi.org/10.1289/ehp.1103667>,  
669 2012.
- 670 Bondy, S. C.: Anthropogenic pollutants may increase the incidence of neurodegenerative disease in an aging population,  
671 *Toxicology*, 341–343, 41–46, <https://doi.org/10.1016/j.tox.2016.01.007>, 2016.
- 672 Borlaza, L. J. S., Weber, S., Uzu, G., Jacob, V., Cañete, T., Micallef, S., Trébuchon, C., Slama, R., Favez, O., and Jaffrezo,  
673 J.-L.: Disparities in particulate matter (PM<sub>10</sub>) origins and oxidative potential at a city scale (Grenoble, France) – Part 1:  
674 Source apportionment at three neighbouring sites, *Atmos. Chem. Phys.*, 21, 5415–5437, [https://doi.org/10.5194/acp-21-](https://doi.org/10.5194/acp-21-5415-2021)  
675 5415-2021, 2021a.
- 676 Borlaza, L. J. S., Weber, S., Jaffrezo, J.-L., Houdier, S., Slama, R., Rieux, C., Albinet, A., Micallef, S., Trébluchon, C., and  
677 Uzu, G.: Disparities in particulate matter (PM<sub>10</sub>) origins and oxidative potential at a city scale (Grenoble, France) – Part  
678 2: Sources of PM<sub>10</sub> oxidative potential using multiple linear regression analysis and the predictive applicability of  
679 multilayer perceptron neural network analysis, *Atmos. Chem. Phys.*, 21, 9719–9739, [https://doi.org/10.5194/acp-21-](https://doi.org/10.5194/acp-21-9719-2021)  
680 9719-2021, 2021b.
- 681 Borlaza, L. J., Weber, S., Marsal, A., Uzu, G., Jacob, V., Besombes, J.-L., Chatain, M., Conil, S., and Jaffrezo, J.-L.: Nine-  
682 year trends of PM<sub>10</sub> sources and oxidative potential in a rural background site in France, *Atmos. Chem. Phys.*, 22,  
683 8701–8723, <https://doi.org/10.5194/acp-22-8701-2022>, 2022.
- 684 Borm, P. J. A., Kelly, F., Künzli, N., Schins, R. P. F., and Donaldson, K.: Oxidant generation by particulate matter: from  
685 biologically effective dose to a promising, novel metric, *Occup. Environ. Med.*, 64, 73–74,  
686 <https://doi.org/10.1136/oem.2006.029090>, 2007.
- 687 Calas, A., Uzu, G., Martins, J. M. F., Voisin, D., Spadini, L., Lacroix, T., and Jaffrezo, J.-L.: The importance of simulated  
688 lung fluid (SLF) extractions for a more relevant evaluation of the oxidative potential of particulate matter, *Sci. Rep.* 7,  
689 11617, <https://doi.org/10.1038/s41598-017-11979-3>, 2017.

690 Calas, A., Uzu, G., Kelly, F. J., Houdier, S., Martins, J. M. F., Thomas, F., Molton, F., Charron, A., Dunster, C., Oliete, A.,  
691 Jacob, V., Besombes, J.-L., Chevrier, F., and Jaffrezo, J.-L.: Comparison between five acellular oxidative potential  
692 measurement assays performed with detailed chemistry on PM<sub>10</sub> samples from the city of Chamonix (France), *Atmos.*  
693 *Chem. Phys.*, 18, 7863–7875, <https://doi.org/10.5194/acp-18-7863-2018>, 2018.

694 Calas, A., Uzu, G., Besombes, J.-L., Martins, J. M. F., Redaelli, M., Weber, S., Charron, A., Albinet, A., Chevrier, F.,  
695 Brulfert, G., Mesbah, B., Favez, O., and Jaffrezo, J.-L.: Seasonal variations and chemical predictors of oxidative  
696 potential (OP) of particulate matter (PM), for seven urban French sites, *Atmosphere*, 10, 698,  
697 <https://doi.org/10.3390/atmos10110698>, 2019.

698 Cassee, F. R., Héroux, M.-E., Gerlofs-Nijland, M. E., and Kelly, F. J.: Particulate matter beyond mass: recent health  
699 evidence on the role of fractions, chemical constituents and sources of emission, *Inhal. Toxicol.*, 25, 802–812,  
700 <https://doi.org/10.3109/08958378.2013.850127>, 2013.

701 Cavalli, F., Viana, M., Yttri, K. E., Genberg, J., and Putaud, J.-P.: Toward a standardised thermal-optical protocol for  
702 measuring atmospheric organic and elemental carbon: the EUSAAR protocol, *Atmos. Meas. Tech.*, 3, 79–89,  
703 <https://doi.org/10.5194/amt-3-79-2010>, 2010.

704 Charrier, J. G. and Anastasio, C.: On dithiothreitol (DTT) as a measure of oxidative potential for ambient particles: evidence  
705 for the importance of soluble transition metals, *Atmos. Chem. Phys.*, 12, 9321–9333, <https://doi.org/10.5194/acp-12-9321-2012>, 2012.

707 Charrier, J. G., McFall, A. S., Vu, K. K.-T., Baroi, J., Olea, C., Hasson, A., and Anastasio, C.: A Bias in the “Mass-  
708 Normalized” DTT Response – An Effect of Non-Linear Concentration-Response Curves for Copper and Manganese,  
709 *Atmos. Environ.*, 144, 325–334, <https://doi.org/10.1016/j.atmosenv.2016.08.071>, 2016.

710 Chiari, M., Yubero, E., Calzolari, G., Lucarelli, F., Crespo, J., Galindo, N., Nicolás, J. F., Giannoni, M., and Nava, S.:  
711 Comparison of PIXE and XRF analysis of airborne particulate matter samples collected on Teflon and quartz fibre  
712 filters, *Nucl. Instrum. Meth. B*, 417, 128–132, <https://doi.org/10.1016/j.nimb.2017.07.031>, 2018.

713 Chirizzi, D., Cesari, D., Guascito, M. R., Dinoi, A., Giotta, L., Donateo, A., and Contini, D.: Influence of Saharan dust  
714 outbreaks and carbon content on oxidative potential of water-soluble fractions of PM<sub>2.5</sub> and PM<sub>10</sub>, *Atmos. Environ.*,  
715 163, 1–8, <https://doi.org/10.1016/j.atmosenv.2017.05.021>, 2017.

716 Cho, A. K., Sioutas, C., Miguel, A. H., Kumagai, Y., Schmitz, D. A., Singh, M., Eiguren-Fernandez, A., and Froines, J. R.:  
717 Redox activity of airborne particulate matter at different sites in the Los Angeles Basin, *Environ. Res.*, 99, 40–47,  
718 <https://doi.org/10.1016/j.envres.2005.01.003>, 2005.

719 Cohen, A., Brauer, M., Burnett, R., Anderson, H., Frostad, J., Estep, K., Balakrishnan, K., Brunekreef, B., Dandona, L.,  
720 Dandona, R., Feigin, V., Freedman, G., Hubbell, B., Jobling, A., Kan, H., Knibbs, L., Liu, Y., Martin, R., Morawska,  
721 L., and Forouzanfar, M.: Estimates and 25-year trends of the global burden of disease attributable to ambient air  
722 pollution: An analysis of data from the Global Burden of Diseases Study 2015, *The Lancet*, 389, 1907–1918,  
723 [https://doi.org/10.1016/S0140-6736\(17\)30505-6](https://doi.org/10.1016/S0140-6736(17)30505-6), 2017.

724 Daellenbach, K. R., Uzu, G., Jiang, J., Cassagnes, L.-E., Leni, Z., Vlachou, A., Stefanelli, G., Canonaco, F., Weber, S.,  
725 Segers, A., Kuenen, J. J. P., Schaap, M., Favez, O., Albinet, A., Aksoyoglu, S., Dommen, J., Baltensperger, U., Geiser,  
726 M., El Haddad, I., Jaffrezo, J.-L., and Prévôt, A. S. H.: Sources of particulate-matter air pollution and its oxidative  
727 potential in Europe, *Nature*, 587, 414–419, <https://doi.org/10.1038/s41586-020-2902-8>, 2020.

728 Dhalla, N., Temsah, R. M., and Neticadan, Th.: Role of oxidative stress in cardiovascular diseases, *J. Hypertens.*, 18,  
729 [https://doi.org/655–673](https://doi.org/655-673), 10.1097/00004872-200018060-00002, 2000.

730 Dai, Q., Hopke, Ph. K., Bi, X., and Feng, Y.: Improving apportionment of PM<sub>2.5</sub> using multisite PMF by constraining G-  
731 values with a priori information, *Sci. Total Environ.*, 736, 139657, <https://doi.org/10.1016/j.scitotenv.2020.139657>,  
732 2020.

733 Donaldson, K., Tran, L., Jimenez, L., Duffin, R., Newby, D., Mills, N., MacNee, W., and Stone, V.: Combustion-derived  
734 nanoparticles: a review of their toxicology following inhalation exposure, *Part. Fibre Toxicol.*, 2, 10,  
735 <https://doi.org/10.1186/1743-8977-2-10>, 2005.

736 EPA: Positive matrix factorization model for environmental data analyses, [https://www.epa.gov/air-research/positive-](https://www.epa.gov/air-research/positive-matrix-factorization-model-environmental-data-analyses)  
737 [matrix-factorization-model-environmental-data-analyses](https://www.epa.gov/air-research/positive-matrix-factorization-model-environmental-data-analyses), last access: 20 June 2022, 2017.

738 Fang, T., Verma, V., Bates, J. T., Abrams, J., Klein, M., Strickland, M. J., Sarnat, S. E., Chang, H. H., Mulholland, J. A.,  
739 Tolbert, P. E., Russell, A. G., and Weber, R. J.: Oxidative potential of ambient water-soluble PM<sub>2.5</sub> in the southeastern  
740 United States: contrasts in sources and health associations between ascorbic acid (AA) and dithiothreitol (DTT) assays,  
741 *Atmos. Chem. Phys.*, 16, 3865–3879, <https://doi.org/10.5194/acp-16-3865-2016>, 2016.

742 Fang, T., Guo, H., Zeng, L., Verma, V., Nenes, A., and Weber, R. J.: Highly acidic ambient particles, soluble metals, and  
743 oxidative potential: a link between sulfate and aerosol toxicity, *Environ. Sci. Technol.*, 51, 2611–2620,  
744 <https://doi.org/10.1021/acs.est.6b06151>, 2017.

745 Furu, E., Angyal, A., Szoboszlai, Z., Papp, E., Török, Z., and Kertész, Z.: Characterization of aerosol pollution in two  
746 Hungarian cities in winter 2009–2010, *Atmosphere*, 13, 554, <https://doi.org/10.3390/atmos13040554>, 2022.

747 Gao, D., Ripley, S., Weichenthal, S., and Godri Pollitt, K. J.: Ambient particulate matter oxidative potential: chemical  
748 determinants, associated health effects, and strategies for risk management, *Free Radic. Biol. Med.*, 151, 7–25,  
749 <https://doi.org/10.1016/j.freeradbiomed.2020.04.028>, 2020.

750 Godri, K. J., Harrison, R. M., Evans, T., Baker, T., Dunster, C., Mudway, I. S., and Kelly, F. J.: Increased oxidative burden  
751 associated with traffic component of ambient particulate matter at roadside and urban background schools sites in  
752 London, *PLoS One*, 6, 1–11, <https://doi.org/10.1371/journal.pone.0021961>, 2011.

753 Grange, S. K., Uzu, G., Weber, S., Jaffrezo, J.-L., and Hueglin, C.: Linking Switzerland's PM<sub>10</sub> and PM<sub>2.5</sub> oxidative potential  
754 (OP) with emission sources, *Atmos. Chem. Phys.*, 22, 7029–7050, <https://doi.org/10.5194/acp-22-7029-2022>, 2022.

755 Hoffer, A., Tóth, Á., Jancsek-Turóczi, B., Machon, A., Meiramova, A., Nagy, A., Marmureanu, L., and Gelencsér, A.:  
756 Potential new tracers and their mass fraction in the emitted PM<sub>10</sub> from the burning of household waste in stoves,  
757 *Atmos. Chem. Phys.*, 21, 17855–17864, <https://doi.org/10.5194/acp-21-17855-2021>, 2021.

758 Hopke, P. K.: Review of receptor modeling methods for source apportionment, *J. Air. Waste Manag. Assoc.*, 66, 237–259,  
759 <https://doi.org/10.1080/10962247.2016.1140693>, 2016.

760 Hopke, P. K.: A guide to positive matrix factorization, Clarkson University, Potsdam, USA, 2000.

761 In 't Veld, M., Pandolfi, M., Amato, F., Pérez, N., Reche, C., Dominutti, P., Jaffrezo, J.-L., Alastuey, A., Querol, X., and  
762 Uzu, G.: Discovering oxidative potential (OP) drivers of atmospheric PM<sub>10</sub>, PM<sub>2.5</sub>, and PM<sub>1</sub> simultaneously in North-  
763 Eastern Spain, *Sci. Total Environ.*, 857, 159386, <https://doi.org/10.1016/j.scitotenv.2022.159386>, 2023.

764 Janssen, N. A. H., Yang, A., Strak, M., Steenhof, M., Hellack, B., Gerlofs-Nijland, M. E., Kuhlbusch, T., Kelly, F., Harrison,  
765 R., Brunekreef, B., Hoek, G., and Cassee, F.: Oxidative potential of particulate matter collected at sites with different  
766 source characteristics, *Sci. Total Environ.*, 472, 572–581, <https://doi.org/10.1016/j.scitotenv.2013.11.099>, 2014.

767 Katerji, M., Filippova, M., and Duerksen-Hughes, P.: Approaches and methods to measure oxidative stress in clinical  
768 samples: research applications in the cancer field, *Oxidative Med. Cell. Longev.*, 12, 1279250,  
769 <https://doi.org/10.1155/2019/1279250>, 2019.

770 Kelly, F. J. and Mudway, I. S.: Protein oxidation at the air-lung interface, *Amino Acids*, 25, 375–396,  
771 <https://doi.org/10.1007/s00726-003-0024-x>, 2003.

772 Kelly, F. J. and Fussell, J. C.: Size, source and chemical composition as determinants of toxicity attributable to ambient  
773 particulate matter, *Atmos. Environ.*, 60, 504–526, <https://doi.org/10.1016/j.atmosenv.2012.06.039>, 2012.

774 Kelly, F. J. and Fussell, J. C.: Air pollution and public health: emerging hazards and improved understanding of risk,  
775 *Environ. Geochem. Health*, 37, 631–649, <https://doi.org/10.1007/s10653-015-9720-1>, 2015.

776 Kelly, F. J. and Fussell, J. C.: Toxicity of airborne particles-established evidence, knowledge gaps and emerging areas of  
777 importance, *Philos. Trans. R. Soc.*, A378, 2019.0322, <https://doi.org/10.1098/rsta.2019.0322>, 2020.

778 Kodros, J. K., Papanastasiou, D. K., Paglione, M., Masiol, M., Squizzato, S., Florou, K., Skyllakou, K., Kaltsonoudis, Ch.,  
779 Nenes, A., and Pandis, S. N.: Rapid dark aging of biomass burning as an overlooked source of oxidized organic aerosol,  
780 *Proc. Natl. Acad. Sci. USA*, 117, 33028–33033, <https://doi.org/10.1073/pnas.2010365117>, 2020.

781 Kurihara, K., Iwata, A., Murray Horwitz, S. G., Ogane, K., Sugioka, T., Matsuki, A., and Okuda, T.: Contribution of  
782 physical and chemical properties to dithiothreitol-measured oxidative potentials of atmospheric aerosol particles at  
783 urban and rural sites in Japan, *Atmosphere*, 13, 319, <https://doi.org/10.3390/atmos13020319>, 2022.

784 Künzli, N., Mudway, I. S., Gotschi, T., Shi, T. M., Kelly, F. J., Cook, S., Burney, P., Forsberg, B., Gauderman, J. W.,  
785 Hazenkamp, M. E., Heinrich, J., Jarvis, D., Norback, D., Payo-Losa, F., Poli, A., Sunyer, J., and Borm, P. J. A.:  
786 Comparison of oxidative properties, light absorbance, and total and elemental mass concentration of ambient PM<sub>2.5</sub>  
787 collected at 20 European sites, *Environ. Health Perspect.*, 114, 684–690, <https://doi.org/10.1289/ehp.8584>, 2006.

788 Lelieveld, J., Evans, J. S., Fnais, M., Giannadaki, D., and Pozzer, A.: The contribution of outdoor air pollution sources to  
789 premature mortality on a global scale, *Nature*, 525, 367–371, <https://doi.org/10.1038/nature15371>, 2015.

790 Lelieveld, J., Pozzer, A., Pöschl, U., Fnais, M., Haines, A., and Münzel, T.: Loss of life expectancy from air pollution  
791 compared to other risk factors: a worldwide perspective, *Cardiovasc. Res.*, 116, 1910–1917,  
792 <https://doi.org/10.1093/cvr/cvaa073>, 2020.

793 Lionetto, M. G., Guascito, M. R., Giordano, M. E., Caricato, R., De Bartolomeo, A. R., Romano, M. P., Conte, M., Dinoi,  
794 A., and Contini, D.: Oxidative potential, cytotoxicity, and intracellular oxidative stress generating capacity of PM<sub>10</sub>: a  
795 case study in south of Italy, *Atmosphere*, 12, 464, <https://doi.org/10.3390/atmos12040464>, 2021.

796 Norris, G., Duvall, R., Brown, S., and Bai, S.: EPA Positive Matrix Factorization (PMF) 5.0 fundamentals and user guide,  
797 Technical Report, U.S. Environmental Protection Agency, National Exposure Research Laboratory, Washington, USA,  
798 2014.

799 Paatero, P. and Tapper, U.: Positive matrix factorization: A non-negative factor model with optimal utilization of error  
800 estimates of data values, *Environmetrics*, 5, 111–126, <https://doi.org/10.1002/env.3170050203>, 1994.

801 Pye, H. O. T., Ward-Caviness, C. K., Murphy, B. N., Appel, K. W., and Seltzer, K. M.: Secondary organic aerosol  
802 association with cardiorespiratory disease mortality in the United States, *Nat. Commun.*, 12, 7215,  
803 <https://doi.org/10.1038/s41467-021-27484-1>, 2021.

804 Riediker, M., Zink, D., Kreyling, W., Oberdörster, G., Elder, A., Graham, U., Lynch, I., Duschl, A., Ichihara, G., Ichihara,  
805 S., Kobayashi, T., Hisanaga, N., Umezawa, M., Cheng, T. J., Handy, R., Gulumian, M., Tinkle, S., and Cassee, F.:  
806 Particle toxicology and health - where are we?, *Part. Fibre Toxicol.*, 16, 19, <https://doi.org/10.1186/s12989-019-0302-8>,  
807 2019.

808 Salma, I., Chi, X., and Maenhaut, W.: Elemental and organic carbon in urban canyon and background environments in  
809 Budapest, Hungary, *Atmos. Environ.*, 38, 27–36, <https://doi.org/10.1016/j.atmosenv.2003.09.047>, 2004.

810 Salma, I., Ocskay, R., Raes, N., and Maenhaut, W.: Fine structure of mass size distributions in urban environment, *Atmos.*  
811 *Environ.*, 39, 5363–5374, <https://doi.org/10.1016/j.atmosenv.2005.05.021>, 2005.

812 Salma, I., Németh, Z., Weidinger, T., Kovács, B., and Kristóf, G.: Measurement, growth types and shrinkage of newly  
813 formed aerosol particles at an urban research platform, *Atmos. Chem. Phys.*, 16, 7837–7851,  
814 <https://doi.org/10.5194/acp-16-7837-2016>, 2016.

815 Salma, I., Vasánits-Zsigrai, A., Machon, A., Varga, T., Major, I., Gergely, V., and Molnár, M.: Fossil fuel combustion,  
816 biomass burning and biogenic sources of fine carbonaceous aerosol in the Carpathian Basin, *Atmos. Chem. Phys.*, 20,  
817 4295–4312, <https://doi.org/10.5194/acp-20-4295-2020>, 2020a.

818 Salma, I., Vörösmarty, M., Gyöngyösi, A. Z., Thén, W., and Weidinger, T.: What can we learn about urban air quality with  
819 regard to the first outbreak of the COVID-19 pandemic? A case study from central Europe, *Atmos. Chem. Phys.*, 20,  
820 15725–15742, <https://doi.org/10.5194/acp-20-15725-2020>, 2020b.

821 Salma, I., Varga, P. T., Vasánits, A., Machon, A.: Secondary organic carbon and its contributions in different atmospheric  
822 environments of a continental region and seasons, *Atmos. Res.*, 278, 106360,  
823 <https://doi.org/10.1016/j.atmosres.2022.106360>, 2022.

824 Shahpoury, P., Zhang, Z. W., Arangio, A., Celo, V., Dabek-Zlotorzynska, E., Harner, T., and Nenes, A.: The influence of  
825 chemical composition, aerosol acidity, and metal dissolution on the oxidative potential of fine particulate matter and  
826 redox potential of the lung lining fluid, *Environ. Internat.*, 148, 106343, <https://doi.org/10.1016/j.envint.2020.106343>,  
827 2021.

828 Shahpoury, P., Zhang, Z. W., Filippi, A., Hildmann, S., Lelieveld, S., Mashtakov, B., Patel, B. R., Traub, A., Umbrio, D.,  
829 Wietzorek, M., Wilson, J., Berkemeier, T., Celo, V., Dabek-Zlotorzynska, E., Evans, G., Harner, T., Kerman, K.,  
830 Lammel, G., Noorozifar, M., Pöschl, U., and Tong, H.: Inter-comparison of oxidative potential metrics for airborne  
831 particles identifies differences between acellular chemical assays, *Atmos. Pollut. Res.*, 13, 101596,  
832 <https://doi.org/10.1016/j.apr.2022.101596>, 2022.

833 Srivastava, D., Tomaz, S., Favez, O., Lanzafame, G. M., Golly, B., Besombes, J.-L., Alleman, L. Y., Jaffrezo, J.-L., Jacob,  
834 V., Perraudin, E., Villenave, E., and Albinet, A.: Speciation of organic fraction does matter for source apportionment.  
835 Part 1: A one-year campaign in Grenoble (France), *Sci. Total Environ.*, 624, 1598–1611,  
836 <https://doi.org/10.1016/j.scitotenv.2017.12.135>, 2018.

837 Szigeti, T., Óvári, M., Dunster, C., Kelly, F. J., Lucarelli, F., and Záray, G.: Changes in chemical composition and oxidative  
838 potential of urban PM(2.5) between 2010 and 2013 in Hungary, *Sci. Total Environ.*, 518–519, 534–544,  
839 <https://doi.org/10.1016/j.scitotenv.2015.03.025>, 2015.

840 Valavanidis, A., Fiotakis, K., and Vlachogianni, T.: Airborne particulate matter and human health: toxicological assessment  
841 and importance of size and composition of particles for oxidative damage and carcinogenic mechanisms, *J. Environ.*  
842 *Sci. Health C*, 26, 339–362, <https://doi.org/10.1080/10590500802494538>, 2008.

843 Valavanidis, A., Vlachogianni, T., Fiotakis, K., and Loridas, S.: Pulmonary oxidative stress, inflammation and cancer:  
844 respirable particulate matter, fibrous dusts and ozone as major causes of lung carcinogenesis through reactive oxygen  
845 species mechanisms, *Int. J. Environ. Res. Public Health*, 10, 3886–3907, <https://doi.org/10.3390/ijerph10093886>, 2013.

846 Varga, G.: Changing nature of Saharan dust deposition in the Carpathian Basin (Central Europe): 40 years of identified  
847 North African dust events (1979–2018), *Environ. Int.*, 139, 105712, <https://doi.org/10.1016/j.envint.2020.105712>,  
848 2020.

849 Verma, V., Rico-Martinez, R., Kotra, N., King, L., Liu, J., Snell, T. W., and Weber, R. J.: Contribution of water-soluble and  
850 insoluble components and their hydrophobic/hydrophilic subfractions to the reactive oxygen species-generating  
851 potential of fine ambient aerosols, *Environ. Sci. Technol.*, 46, 11384–11392, <https://doi.org/10.1021/es302484r>, 2012

852 Verma, V., Fang, T., Guo, H., King, L., Bates, J. T., Peltier, R. E., Edgerton, E., Russell, A. G., and Weber, R. J.: Reactive  
853 oxygen species associated with water-soluble PM<sub>2.5</sub> in the southeastern United States: spatiotemporal trends and source  
854 apportionment, *Atmos. Chem. Phys.*, 14, 12915–12930, <https://doi.org/10.5194/acp-14-12915-2014>, 2014.

855 Verma, V., Fang, T., Xu, L., Peltier, R. E., Russell, A. G., Ng, N. L., and Weber, R. J.: Organic aerosols associated with the  
856 generation of reactive oxygen species (ROS) by water-soluble PM<sub>2.5</sub>, *Environ. Sci. Technol.*, 49, 4646–4656,  
857 <https://doi.org/10.1021/es505577w>, 2015.

858 Visentin, M., Pagnoni, A., Sarti, E., and Pietrogrande, M. C.: Urban PM<sub>2.5</sub> oxidative potential: Importance of chemical  
859 species and comparison of two spectrophotometric cell-free assays, *Environ. Pollut.*, 219, 72–79,  
860 <https://doi.org/10.1016/j.envpol.2016.09.047>, 2016.

861 Wang, S., Ye, J., Soong, R., Wu, B., Yu, L., Simpson, A. J., and Chan, A. W. H.: Relationship between chemical  
862 composition and oxidative potential of secondary organic aerosol from polycyclic aromatic hydrocarbons, *Atmos.*  
863 *Chem. Phys.*, 18, 3987–4003, <https://doi.org/10.5194/acp-18-3987-2018>, 2018.

864 Weichenthal, S., Shekarrizfard, M., Traub, A., Kulka, R., Al-Rijleh, K., Anowar, S., Evans, G., and Hatzopoulou, M.:  
865 Within-city spatial variations in multiple measures of PM<sub>2.5</sub> oxidative potential in Toronto, Canada, *Environ. Sci.*  
866 *Technol.*, 53, 2799–2810, <https://doi.org/10.1021/acs.est.8b05543>, 2019.

867 Weber, S., Uzu, G., Calas, A., Chevrier, F., Besombes, J.-L., Charron, A., Salameh, D., Ježek, I., Močnik, G., and Jaffrezo,  
868 J.-L.: An apportionment method for the oxidative potential of atmospheric particulate matter sources: application to a  
869 one-year study in Chamonix, France, *Atmos. Chem. Phys.*, 18, 9617–9629, <https://doi.org/10.5194/acp-18-9617-2018>,  
870 2018.

871 Weber, S., Uzu, G., Favez, O., Borlaza, L. J. S., Calas, A., Salameh, D., Chevrier, F., Allard, J., Besombes, J.-L., Albinet, A.,  
872 Pontet, S., Mesbah, B., Gille, G., Zhang, S., Pallares, C., Leoz-Garziandia, E., and Jaffrezo, J.-L.: Source  
873 apportionment of atmospheric PM<sub>10</sub> oxidative potential: synthesis of 15 year-round urban datasets in France, *Atmos.*  
874 *Chem. Phys.*, 21, 11353–11378, <https://doi.org/10.5194/acp-21-11353-2021>, 2021.

875 Wong, J. P. S., Tsagkaraki, M., Tsiotra, I., Mihalopoulos, N., Violaki, K., Kanakidou, M., Sciare, J., Nenes, A., and Weber,  
876 R. J.: Effects of atmospheric processing on the oxidative potential of biomass burning organic aerosols, *Environ. Sci.*  
877 *Technol.*, 53, 6747–6756, <https://doi.org/10.1021/acs.est.9b01034>, 2019.

878 Yang, A., Hellack, B., Leseman, D., Brunekreef, B., Kuhlbusch, T. A., Cassee, F. R., Hoek, G., and Janssen, N. A.:  
879 Temporal and spatial variation of the metal-related oxidative potential of PM<sub>2.5</sub> and its relation to PM<sub>2.5</sub> mass and  
880 elemental composition, *Atmos. Environ.*, 102, 62–69, <https://doi.org/10.1016/j.atmosenv.2014.11.053>, 2015.

881 Yu, S., Liu, W., Xu, Y., Yi, K., Zhou, M., Tao, S., and Liu, W.: Characteristics and oxidative potential of atmospheric PM<sub>2.5</sub>  
882 in Beijing: Source apportionment and seasonal variation, *Sci. Total Environ.*, 650, 277–287,  
883 <https://doi.org/10.1016/j.scitotenv.2018.09.021>, 2019.

884 Yue, Y., Chen, H., Setyan, A., Elser, M., Dietrich, M., Li, J., Zhang, T., Zhang, X., Zheng, Y., Wang, J., and Yao, M.: Size-  
885 resolved endotoxin and oxidative potential of ambient particles in Beijing and Zürich, *Environ. Sci. Technol.*, 52,  
886 6816–6824, <https://doi.org/10.1021/acs.est.8b01167>, 2018.

887 Zhang, Z.-H., Hartner, E., Uttinger, B., Gfeller, B., Paul, A., Sklorz, M., Czech, H., Yang, B. X., Su, X. Y., Jakobi, G.,  
888 Orasche, J., Schnelle-Kreis, J., Jeong, S., Gröger, T., Pardo, M., Hohaus, T., Adam, T., Kiendler-Scharr, A., Rudich, Y.,  
889 Zimmermann, R., and Kalberer, M.: Are reactive oxygen species (ROS) a suitable metric to predict toxicity of  
890 carbonaceous aerosol particles?, *Atmos. Chem. Phys.*, 22, 1793–1809, <https://doi.org/10.5194/acp-22-1793-2022>, 2022.